Important factors for the formation of radical cation of stilbene and substituted stilbenes during resonant two-photon ionization with a 266- or 355-nm laser

Shingo Samori, Michihiro Hara, Sachiko Tojo, Mamoru Fujitsuka, Tetsuro Majima[*]

The Institute of Scientific and Industrial Research (SANKEN), Osaka University, Mihogaoka 8-1, Ibaraki, Osaka 567-0047, Japan

Abstract

The resonant two-photon ionization (TPI) of *trans*-stilbene and substituted *trans*-stilbenes (**S**) in acetonitrile was studied by laser flash photolysis using a Nd^{3+}:YAG laser (266- or 355-nm). The transient absorption spectra of **S** radical cations ($S^{\bullet+}$) with a peak around 450–540 nm were observed. Formation of $S^{\bullet+}$ can be explained by two-step two-photon excitation from the ground state (S_0) to the lowest singlet excited state (S_1) and from the S_1 to the higher singlet excited state (S_n), from which ionization occurs. The formation quantum yield of $S^{\bullet+}$ (ϕ_{ion}) was 0.005–0.11. Little or no relation between ϕ_{ion} and E^{ox} was observed for non-substituted (**1**), mono-*p*-substituted (**2–7**) and di-*p*-substituted (**8–11**), methoxy-substituted (**12–16**), and donor–acceptor-*p*-substituted *trans*-stilbenes (**17–21**). On the other hand, ϕ_{ion} increased with the increase of the fluorescence lifetime (τ_f) for all **S**. Interestingly, relatively large ϕ_{ion} was observed for **17–21** even though they have relatively short τ_f among those of **S**. It is suggested that the CT electronic character of the S_1 state and, therefore, the large molar absorption coefficient are responsible for the efficient TPI of **17–21**.
© 2005 Elsevier B.V. All rights reserved.

Keywords: Radical cation; Stilbene; Resonant two-photon ionization; Nd^{3+}:YAG laser photolysis; Substituent effect; Property of the singlet excited state
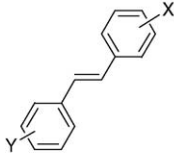
1. Introduction

Photophysical properties of the lowest singlet state (S_1) have been extensively studied with relation to the efficient two-photon ionization (TPI). For example, pyrene (Py) and substituted Py, of which the S_1 states have sufficiently long fluorescence lifetimes (τ_f) in the range of a few tens of nanoseconds, undergo the efficient TPI during the laser photolysis using an intense short-pulsed laser at a sufficiently high fluence (*F*) [1–4]. The TPI of the molecules with a relatively long τ_f such as diarylmethylhalides [5] and Py, the TPI of *trans*-stilbene (**1**) with a short τ_f has been studied by means of picoseconds pump-probe CARS [6–10] and picoseconds time-resolved Raman spectral measurement [11]. Recently, we have reported the

TPI of **1** and methoxy-substituted *trans*-stilbenes (**12–16**) in acetonitrile (AN) by laser flash photolysis (LFP) using a XeCl excimer laser (308 nm, $F = 0.51$ J cm^{-2}, 25-ns FWHM, $P = 2.0 \times 10^7$ J cm^{-2} s^{-1}) [12]. A high ionization yield (ϕ_{ion}) was observed in the TPI of *trans*-4,4′-dimethoxystilbene (**16**) with the long τ_f among **1** and **12–16**, suggesting the quinoid-type electronic structure involving π-electrons and *n*-electrons of the oxygen atoms of two methoxy substituents of **16** in the S_1 state. A high ionization yield was also observed in the TPI of *trans*-3,5-dimethoxystilbene (**15**) with a relatively high oxidation potential and a long τ_f. This is explained by the intermediary of the S_1 state with the intramolecular charge-transfer (CT) nature for the TPI.

In order to clarify the TPI of **1** and substituted *trans*-stilbenes (**S**), we have studied systematically the TPI of five types of *trans*-stilbenes (**S**): non-substituted (**1**), mono-*p*-substituted (**2–7**), di-*p*-substituted (**8–11**) and methoxy-substituted *trans*-stilbenes (**12–16**), and *trans*-stilbenes sub-

* Corresponding author. Tel.: +81 6 6879 8495; fax: +81 6 6879 8499.
 E-mail address: majima@sanken.osaka-u.ac.jp (T. Majima).

S	X	Y
1	H	H
2	4-F	H
3	4-Cl	H
4	4-Br	H
5	4-CH$_3$	H
6	4-CF$_3$	H
7	4-CN	H
8	4-F	4-F
9	4-Cl	4-Cl
10	4-Br	4-Br
11	4-CH$_3$	4-CH$_3$
12	4-CH$_3$O	H
13	2,4-(CH$_3$O)$_2$	H
14	3,4-(CH$_3$O)$_2$	H
15	3,5-(CH$_3$O)$_2$	H
16	4-CH$_3$O	4-CH$_3$O
17	4-CH$_3$O	4-Cl
18	4-CH$_3$O	4-Br
19	4-CH$_3$O	4-CO$_2$Et
20	4-CH$_3$O	4-CF$_3$
21	4-CH$_3$O	4-CN

Scheme 1. *trans*-Stilbenes substituted with X and Y (**S**).

stituted with donor and acceptor groups (donor–acceptor-*p*-substituted *trans*-stilbenes, **17**–**21**) (Scheme 1). Air-saturated acetonitrile (AN) solutions of **S** were irradiated using a Nd^{3+}:YAG laser at 266 ($F = 0.10 \, \text{J cm}^{-2}$, 5-ns FWHM, $P = 2.0 \times 10^7 \, \text{J cm}^{-2} \, \text{s}^{-1}$) or 355 nm ($F = 0.31 \, \text{J cm}^{-2}$, 5-ns FWHM, $P = 6.0 \times 10^7 \, \text{J cm}^{-2} \, \text{s}^{-1}$). Particular interest is focused on the elucidation of important factors, which govern the formation efficiency of **S** radical cations (**S$^{\bullet+}$**). We also investigated the laser wavelength dependence on the TPI efficiency using the 266- and 355-nm lasers. Based on the experimental results, it is found that the TPI of **S** depends strongly on the photophysical properties of **S** in the ground sate (**S**(S$_0$)) and **S**(S$_1$) such as ionization potential (I.P.), fluorescence lifetime, transition probabilities for the excitation of **S**(S$_0$) to **S**(S$_1$), and **S**(S$_1$) to **S** in the S$_n$ state (**S**(S$_n$)).

2. Experimental

2.1. Materials

trans-Stilbene (**1**) (>99.5%) was purchased from Tokyo Kasei and purified by recrystallization from ethanol before use. The substituted *trans*-stilbenes (**2**–**21**) were synthesized by the Wittig reactions of the corresponding substituted benzaldehyde and benzyltriphenylphosphonium chloride with sodium ethoxide in absolute ethanol at room temperature according to the literature [13–23]. **18** was recrystallized from ethyl acetate [13] and others were recrystallized from ethanol before use [14–23]. Acetonitrile (AN) and cyclohexane (CH) (Nacalai Tesque, spectroscopic grade) were used without further purification. Benzophenone (BP), 9,10-dicyanoanthracene (DCA), and biphenyl were purchased from Nacalai Tesque, Aldrich, and Wako, respectively, and purified by recrystallization.

2.2. Absorption and fluorescence spectral measurements

UV absorption spectra were measured in AN with a Shimadzu UV-3100PC UV/visible spectrophotometer. Fluorescence spectra were measured by a Hitachi 850 spectrofluorometer.

2.3. Fluorescence lifetime measurements

Fluorescence lifetimes were measured by the single photon counting method using a streakscope (Hamamatsu Photonics, C4334-01) equipped with a polychromator (Acton Research, SpectraPro150). Femtosecond laser pulse was generated with a broad-band (700–1000-nm) tunable mode-locked Ti:sapphire laser (Spectra-Physics, Tsunami 3941-M1BB, FWHM 100 fs) pumped with a diode laser-pumped solid state laser (Spectra-Physics, Millennia VIIIs). This laser system is tunable in the 700–1000-nm range. For the excitation of samples, the output of the Ti:sapphire laser was converted to the third harmonic oscillation (300 nm) with a harmonic generator (Spectra-Physics, GWU-23FL).

2.4. Nanosecond laser flash photolysis

Nanosecond laser flash photolysis experiments were carried out using the fourth harmonic oscillation (266 nm) or the third harmonic oscillation (355 nm) of a nanosecond Nd^{3+}:YAG laser (Continuum Surelite laser; 5-ns FWHM) as an excitation source. The laser fluence (F) was 0.10 and 0.31 J cm^{-2} at 266 and 355 nm, respectively. The monitor light was obtained from a 450-W Xe lamp (Osram, XBO-450) synchronized with the laser flash. The laser beam was perpendicular to the monitor light. The intensity of the monitor light source was detected using a silicon detector (Hamamatsu Photonics, S5343). The signal from the silicon detector was digitalized by an oscilloscope and transmitted to a personal computer via the RS 232C interface. Transient absorption spectra were measured by a streak camera (Hamamatsu Photonics C7700) equipped with a CCD camera (Hamamatsu Photonics C4742-98). Air-saturated acetonitrile solutions were contained in a transparent rectangular quartz cell (1.0 cm × 1.0 cm × 4.0 cm, path length of 1.0 cm) at room temperature. The absorbance of **S** in ground state was adjusted to be 1.0 at the excitation laser wavelength (266- or 355-nm).

2.5. Oxidation potential measurement

Oxidation potentials (E^{ox}) were measured with cyclic voltammetry (BAS, CV-50W) with platinum working and auxiliary electrodes and an Ag/Ag$^+$ reference electrode at a scan rate of 50 mV s^{-1}. Ferrocene ($E^{ox} = 0.76$ V) was used as an internal standard. Measurements were performed in dry AN containing 1.0×10^{-3} M of **S** and 0.1 M tetraethylammonium tetrafluoroborate.

All spectroscopic and electrochemical measurements were carried out at room temperature (21 °C).

3. Results

3.1. Photophysical properties of S(S₀) and S(S₁)

It is clearly expected that the TPI of **S** depends strongly on the photophysical properties of $S(S_0)$ and $S(S_1)$. Although the former can be directly determined, the latter is not easily accessible. In order to evaluate easily the correlation between the ionization quantum yield and properties of $S(S_0)$ and $S(S_1)$, the photophysical properties were summarized here.

The ground-state absorption peaks of **S** in AN and CH were observed at 286–332 nm with a little influence of the solvent polarity, while the fluorescence peaks were at 350–436 nm with a large shift depending on the solvent polarity (Fig. 1). The Stokes shifts were $(3.7–7.1) \times 10^3$ cm^{-1} and $(2.6–7.9) \times 10^3$ cm^{-1} in AN and CH, respectively. The experimental values are summarized in Table 1. The fluorescence from **2** and **6** was not detected, indicating τ_f of **2** and **6** were shorter than the time-resolution of the experimental apparatus. For methoxy-substituted (**12–16**) and donor–acceptor-p-substituted *trans*-stilbenes (**17–21**), the Stokes shifts in AN were larger than those in CH. In particular, the differences of the Stokes shifts between in AN and in CH ($\Delta\bar{\nu}_{AN} - \Delta\bar{\nu}_{CH}$) were much larger for **15**, **19**, and **21** ($>2.0 \times 10^3$ cm^{-1}) than for others ($<1.5 \times 10^3$ cm^{-1}). These results indicate the relatively large conformational change between S₀ and S₁ states in the cases of **15**, **19**, and **21**. For **15** and **16**, τ_f values were 9100 and 380 ps, respectively, which are longer than others. The long τ_f of **15** and **16** are attributed to the electronic structural change in the S₁ state [12].

3.2. Ionization potentials of S in AN (I.P.AN)

Since the TPI depends on the photon energy and I.P., the I.P. values were estimated from the oxidation potentials.

The cyclic voltagrams (CVs) of most aromatic compounds exhibit irreversible oxidation peaks at scan rate <100 V s^{-1}, with the exception of highly condensed polycyclic compounds [24]. This is shown by the absence of the cathodic component on the return potential scan, largely owing to competition from fast follow-up reactions of metastable radical cations of the aromatic compounds. This irreversible oxidation peaks were also observed for all **S**. Therefore, the peak potentials were summarized as E^{ox}, 0.73–1.39 V, in Table 1. The E^{ox} values of non-substituted (**1**), mono-p-substituted (**2–7**), and di-p-substituted *trans*-stilbenes (**8–11**) were 1.2 ± 0.2 V. In contrast, those of methoxy-substituted (**12–16**) and donor–acceptor-p-substituted *trans*-stilbenes (**17–21**) were lower than 1.02 V except for **15**. The E^{ox} values of **6** and **7** were higher than others. Ionization potential of **S** in AN (I.P.AN) is estimated using Eq. (1) [25,26]:

$$\text{I.P.}_{AN} = \text{I.P.}_{\cdot gas} - E_{AN} = (1.473 \pm 0.027)E^{ox}$$
$$+ (5.821 \pm 0.009) - E_{AN}, \quad (1)$$

where I.P.$_{gas}$ is ionization potential in the gas phase, E_{AN} is the stabilization energy of solvated electron in AN. The I.P.$_{gas}$ values of **S** were calculated to be 6.90–7.87 eV from I.P.$_{gas} = (1.473 \pm 0.027)E^{ox} + (5.821 \pm 0.009)$. The E_{AN} value of **S** in AN was estimated to be 1.9 eV from the absorption peak of solvated electron observed at 660 nm in AN [26]. Thus, I.P.AN of **S** in AN were calculated as shown in Table 2, indicating that the two-photon energies at 266-nm (4.7 eV) or 355-nm (3.5 eV) are sufficient for the TPI of **S**.

3.3. Transient absorption measurement of S•+ during the TPI of S

A transient absorption spectrum with a peak (λ_{max}) at 485 nm was observed during the 266-nm, 5-ns laser flash photolysis of **12** ($F = 0.10$ J cm^{-2}) in air-saturated AN (3.0×10^{-4} M) (Fig. 2). According to the previous report, the transient absorption spectrum observed with two typical absorption peaks at 485 and 780 nm, assigned to the **12** radical cation (**12**•+) [12]. Two peaks are assigned to the $D_2 \leftarrow D_0$ and $D_1 \leftarrow D_0$ transitions, respectively [27].
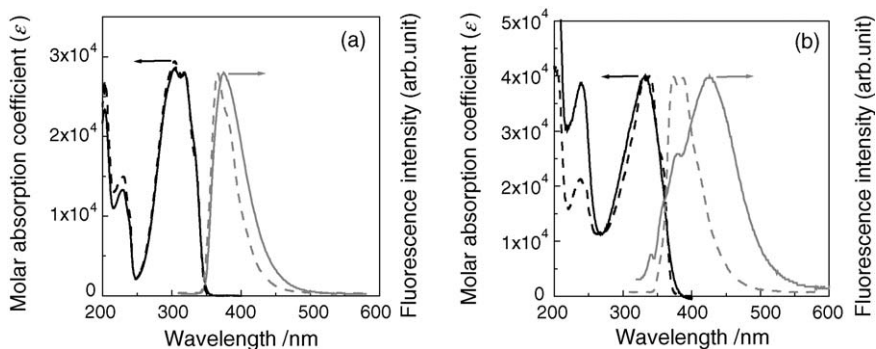

Fig. 1. Absorption and fluorescence spectra of **12** (a) and **21** (b) in AN (solid curves) and CH (dashed curves) solutions.

Table 1
Properties of **S**: ground-state absorption and fluorescence spectral data in acetonitrile (AN) or cyclohexane (CH) solutions, oxidation potentials (E^{ox}), and ionization potentials in AN (I.P.$_{AN}$)

S	Absorption		Fluorescence		Stokes shift (10^3 cm^{-1})		E^{ox} (V)	I.P.$_{AN}$ (eV)
	λ_{max} (nm)	ε_{max} (M^{-1} cm^{-1}) in AN	λ_{max} (nm)	τ_f (ps) in AN	$\Delta\bar{v}_{AN}$ in AN	$\Delta\bar{v}_{CH}$ in CH		
1	307	3.3×10^4	350	44	4.0	4.0	1.22	5.72 ± 0.04
2	293	2.2×10^4	350	nd	5.5	6.7	1.20	5.69 ± 0.04
3	312	3.1×10^4	355	66	3.9	5.0	1.23	5.73 ± 0.04
4	313	3.8×10^4	356	57	3.8	5.0	1.23	5.73 ± 0.04
5	311	3.1×10^4	354	45	4.0	5.2	1.11	5.56 ± 0.04
6	309	3.4×10^4	362	nd	4.8	5.3	1.37	5.94 ± 0.05
7	320	4.3×10^4	378	32	4.8	4.0	1.39	5.97 ± 0.05
8	286	2.6×10^4	350	86	6.4	7.9	1.20	5.69 ± 0.04
9	316	3.5×10^4	359	120	3.7	3.9	1.26	5.78 ± 0.04
10	318	4.6×10^4	362	68	3.8	4.1	1.27	5.79 ± 0.04
11	314	3.1×10^4	358	120	3.9	4.0	1.02	5.42 ± 0.04
12	318	2.8×10^4	375	32	4.7	4.0	0.90	5.25 ± 0.03
13	325	2.2×10^4	394	33	5.4	5.0	0.73	5.00 ± 0.03
14	324	2.9×10^4	388	110	5.1	4.0	0.79	5.08 ± 0.03
15	308	2.9×10^4	394	9100	7.1	4.9	1.22	5.72 ± 0.04
16	325	3.0×10^4	376	380	4.2	4.0	0.75	5.03 ± 0.03
17	322	3.7×10^4	381	23	4.9	4.3	0.93	5.29 ± 0.03
18	323	3.7×10^4	385	24	5.0	3.8	0.92	5.28 ± 0.03
19	333	3.3×10^4	436	43	7.1	4.1	0.97	5.35 ± 0.04
20	323	4.0×10^4	380	13	4.7	4.1	1.00	5.39 ± 0.04
21	332	4.0×10^4	426	20	6.6	2.6	1.02	5.42 ± 0.04

Similarly, transient absorption spectra of **S**$^{\bullet+}$ (**1**$^{\bullet+}$–**21**$^{\bullet+}$) with two peaks around 450–540 nm and 650–870 nm were observed (Fig. 2). For example, the absorption spectra of di-methoxy-substituted *trans*-stilbene (**15**) and donor–acceptor-*p*-substituted *trans*-stilbenes (**20** and **21**) are shown in Fig. 2.

These two peaks of **S**$^{\bullet+}$ were confirmed by the transient absorption measurement during pulse radiolyses of **S** in 1,2-dichloroethane [27].

An electron, which is generated together with **S**$^{\bullet+}$, reacts with AN to give an AN radical anion (AN$^{\bullet-}$) or the dimer

Table 2
Transient absorption peak wavelength (λ_{max}) and coefficient of **S**$^{\bullet+}$ (ε_{max}), and the formation quantum yields of **S**$^{\bullet+}$ (ϕ_{ion}) during the 266- and 355-nm TPI of S in AN[a]

S$^{\bullet+}$	λ_{max} (nm)	ε_{max} (M^{-1} cm^{-1})	ϕ_{ion}^{266}	$\phi_{ion}^{355\,[b]}$
1$^{\bullet+}$	472	59600	1.3×10^{-2}	0
2$^{\bullet+}$	475	44000	1.9×10^{-2}	0
3$^{\bullet+}$	488	70000	1.7×10^{-2}	0
4$^{\bullet+}$	493	62000	1.1×10^{-2}	0
5$^{\bullet+}$	483	68000	1.3×10^{-2}	0
6$^{\bullet+}$	465	23000	1.4×10^{-2}	0
7$^{\bullet+}$	478	51000	5.8×10^{-2}	0
8$^{\bullet+}$	480	43000	1.8×10^{-2}	0
9$^{\bullet+}$	502	57000	2.1×10^{-2}	0
10$^{\bullet+}$	510	50000	2.0×10^{-2}	0
11$^{\bullet+}$	495	60600	3.4×10^{-2}	0
12$^{\bullet+}$	485	60600	1.0×10^{-2}	9.4×10^{-3}
13$^{\bullet+}$	475	37000	1.8×10^{-2}	8.9×10^{-3}
14$^{\bullet+}$	475	36000	3.6×10^{-2}	2.5×10^{-2}
15$^{\bullet+}$	498	27000	1.1×10^{-1}	9.3×10^{-3}
16$^{\bullet+}$	531	66000	6.7×10^{-2}	2.4×10^{-2}
17$^{\bullet+}$	497	24000	2.6×10^{-2}	2.3×10^{-2}
18$^{\bullet+}$	500	25000	2.8×10^{-2}	2.1×10^{-2}
19$^{\bullet+}$	485	8300	7.7×10^{-2}	2.8×10^{-2}
20$^{\bullet+}$	468	22000	1.5×10^{-2}	1.3×10^{-2}
21$^{\bullet+}$	478	9700	3.8×10^{-2}	1.8×10^{-2}

[a] The transient absorption peaks of the D$_2$ ← D$_0$ transition (λ_{max}) and molar absorption coefficients (ε_{max}) at the peak wavelength of **S**$^{\bullet+}$ were obtained by the transient absorption measurement during the 266-nm TPI process. Formation quantum yields (ϕ_{ion}) of **S**$^{\bullet+}$ were calculated from Eq. (2).

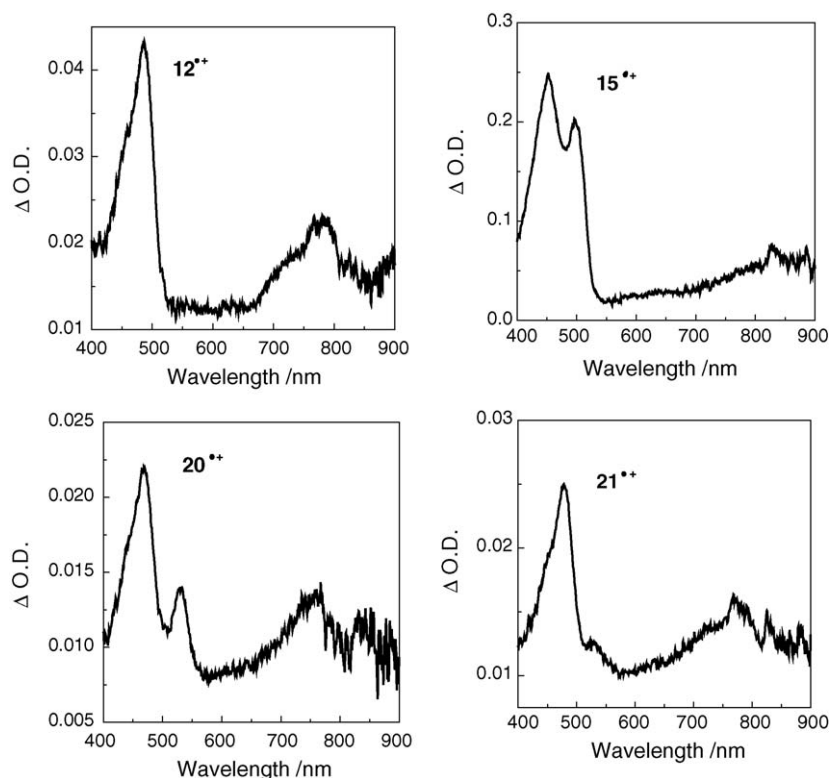[b] No TPI of **1**–**11** occurred because they have no absorbance at 355 nm.

Fig. 2. Transient absorption spectra assigned to **12•+**, **15•+**, **20•+**, and **21•+** observed at the end of a laser flash during the TPI of **S** at 266 nm ($F = 0.10\,\text{J cm}^{-2}$, 5-ns FWHM) in air-saturated AN.

radical anion ($(\text{AN})_2^{\bullet-}$) with a weak absorption in the range of 400–600 nm [28]. Even if the solvated electron in AN reacts partly with **S** at a rate constant of $(2\text{–}5) \times 10^{10}\,\text{M}^{-1}\,\text{s}^{-1}$ [29], **S** radical anion cannot be observed on the time scale of 100 ns under the present experimental condition, since the concentration of **S** was as low as 10^{-4} M. In fact, no transient absorption of **S** radical anions with a peak around 500–550 nm [29] was observed at 100 ns after the laser flash during the TPI of **S** in AN.

3.4. Formation quantum yield of S•+ (φion) of the TPI

The molar absorption coefficients (ε) of **1•+**, **3•+**, **5•+**, **7•+**, and **11•+**–**16•+** have been determined in the previous reports [12,30]. For other **S•+**, the ε values were estimated from the transient absorption peak intensities of **S•+** generated by the hole transfer from biphenyl radical cation ($\varepsilon_{670} = 1.45 \times 10^4\,\text{M}^{-1}\,\text{cm}^{-1}$) [29] during the 355-nm flash photolysis of a mixture of DCA (6.1×10^{-5} M), biphenyl (0.2 M), and **S** in AN.

Furthermore, from optical densities of the transient absorption peak (ΔOD_λ) observed immediately after the 266-nm laser flash and ε values for **S•+**, concentration of **S•+** ([**S•+**]) generated from the 266- and 355-nm TPI of **S** were determined. Using benzophenone in the triplet excited state ($^3\text{BP}^*$) as a chemical actinometer ($\varepsilon_{520} = 6.5 \times 10^3\,\text{M}^{-1}\,\text{cm}^{-1}$), the ϕ_{ion} values were determined

by Eq. (2):

$$\phi_{\text{ion}} = \frac{[\mathbf{S}^{\bullet+}]}{[^3\text{BP}^*]} \qquad (2)$$

The ϕ_{ion} values for **S•+** are also listed in Table 2.

3.5. Relations between φion and E^ox or τf

Figs. 3 and 4 show the relation between ϕ_{ion} and E^{ox} of each type of **S** and all **S**, respectively. Little or no relation between ϕ_{ion} and E^{ox} was observed for all **S**. Fig. 5 shows the relation between ϕ_{ion} and τ_f for **S**. The ϕ_{ion} increased with the increase of τ_f. Each types of **S** showed different slopes. It should be noted that large ϕ_{ion} was obtained for the TPI of **17–21** even though they have short τ_f.

4. Discussion

Oberlé et al. have reported the transient S_1–S_n absorption spectrum of **1** [10]. Similarly, we observed the transient S_1–S_n absorption spectra for **12–21** in a few tens picoseconds time scale during 30-ps laser flash photolysis (Fig. S2). These results indicate the existence of **S**(S_n) level above the ionization limit generated from the secondary excitation of **S**(S_1). Because this S_n state does exist, the photoexcitation occurs from S_1 state, and transient S_1–S_n absorption can be
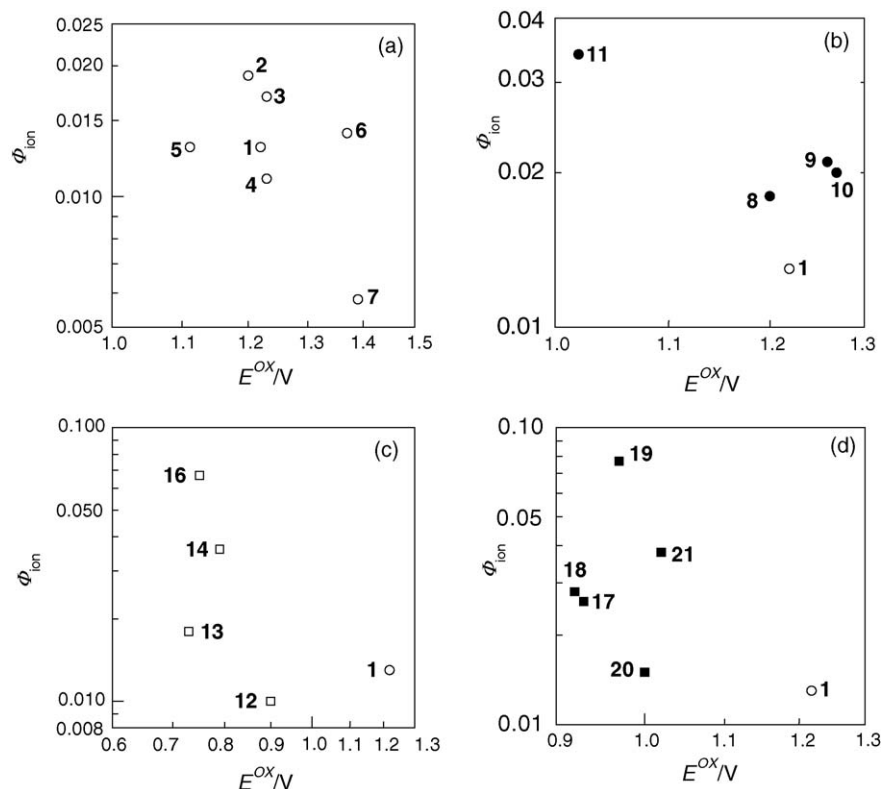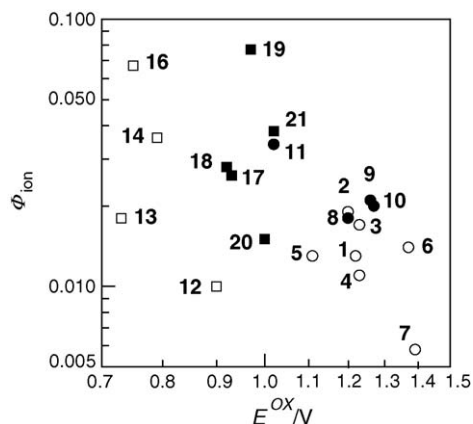
Fig. 3. Plots of log ϕ_{ion} vs. log E^{ox} of non-substituted (**1**, open circle) and mono-*p*-substituted (**2–7**, open circle) (a), di-*p*-substituted (**8–11**, filled circle) (b), methoxy-substituted (**12–14** and **16** open square) (c), and donor–acceptor-*p*-substituted *trans*-stilbenes (**17–21**, filled square) (d) during the TPI with the 266-nm laser flash ($F = 0.10 \, \text{J cm}^{-2}$, 5-ns FWHM). The plots for **15** ($\phi_{ion} = 1.1 \times 10^{-1}$ and $\tau_f = 9100 \, \text{ps}$) were omitted from (c) because τ_f of **15** was much longer than the laser pulse width (5 ns).

observed. In addition, we have reported that a photostationary state of $\mathbf{S}(S_n)$ is attained within the 5-ns laser pulse duration in the TPI of **1** and **12–15** [31]. Consequently, we can suppose that higher $\mathbf{S}(S_n)$ exists with a finite lifetime and undergoes internal conversion to $\mathbf{S}(S_1)$ or ionization to $\mathbf{S}^{\bullet+}$, although the

Fig. 4. Plots of log ϕ_{ion} vs. log E^{ox} of non-substituted (**1**, open circle) and mono-*p*-substituted (**2–7**, open circle) (**1**, di-*p*-substituted (**8–11**, filled circle), methoxy-substituted (**12–14** and **16** open square); donor–acceptor-*p*-substituted *trans*-stilbenes (**17–21**, filled square) during the TPI with the 266-nm laser flash ($F = 0.10 \, \text{J cm}^{-2}$, 5-ns FWHM). Plots of all **S** were shown by one figure.
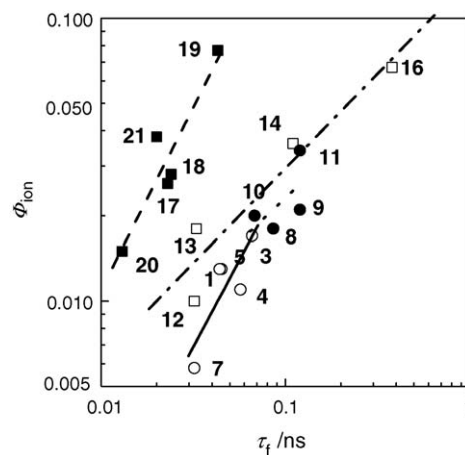

Fig. 5. Plots of log ϕ_{ion} vs. log τ_f for non-substituted and mono-*p*-substituted (**1–7**, open circle), di-*p*-substituted (**8–11**, filled circle), methoxy-substituted (**12–14** and **16**, open square), and donor–acceptor-*p*-substituted *trans*-stilbenes (**17–21**, filled square) on double-logarithmic scales during the TPI with the 266-nm laser flash ($F = 0.10 \, \text{J cm}^{-2}$, 5-ns FWHM). The plots for **2** ($\phi_{ion} = 1.9 \times 10^{-2}$), **6** ($\phi_{ion} = 1.4 \times 10^{-2}$), and **15** ($\phi_{ion} = 1.1 \times 10^{-1}$ and $\tau_f = 9100 \, \text{ps}$) were omitted because τ_f of **2** and **6** were not detected, whereas that of **15** was much longer than the laser pulse width (5 ns).
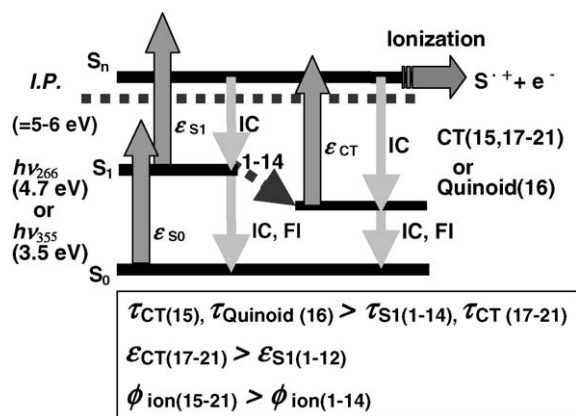
Scheme 2.

secondary excitation of $S(S_1)$ leads to much above the ionization threshold. In other words, $S^{\bullet+}(1^{\bullet+}-21^{\bullet+})$ is generated by the TPI in which S is successively excited to the photostationary state between the S_1 and S_n states by the first- and second-photon excitation, respectively, during the 266-nm, 5-ns laser flash photolysis (Scheme 2).

The concentration of $S^{\bullet+}$ ($[S^{\bullet+}]$) was proportional to the square of laser fluence (F^2) for $1^{\bullet+}$ and $12^{\bullet+}-14^{\bullet+}$ [12]. This relation is usually obtained for the TPI because two-photon absorption is necessary for ionization of S to give $S^{\bullet+}$. Therefore, the two-step two-photon excitation of S is followed by the electron detachment from the S_n state to give $S^{\bullet+}$ and electron during the TPI of S. The TPI of all S is confirmed by the comparison of one-photon and two-photon energies at 266-nm (4.7 eV) or 355-nm (3.5 eV) with the I.P.$_{AN}$ values.

As indicated above ϕ_{ion} depended on τ_f, although no significant relation was found with E^{ox}. The factors governing ϕ_{ion} in the TPI of S are discussed below. In the laser flash photolysis experiments, the absorbance of S in ground state was adjusted to be 1.0 at the excitation laser wavelength; thus, the difference of the transition probability of the S_0–S_1 excitation does not appear in ϕ_{ion}. Therefore, photophysical properties of the S_1 state are expected to be the key factor for ϕ_{ion}.

4.1. Important factors for the TPI of non-substituted (1), mono-p-substituted (2–7), and di-p-substituted trans-stilbenes (8–11)

According to the mechanism of the TPI of S, ϕ_{ion} is expected to increase for S with low E^{ox}, long τ_f, and large transition probabilities of the S_0–S_1 and S_1–S_n excitations. Fig. 3(a and b) show that no significant relation between E^{ox} and ϕ_{ion} in the TPI of 1 (open circle), 2–7 (open circle), and 8–11 (filled circle). It is clearly indicated that τ_f is an important factor for the TPI of 1–11 (Fig. 5). That means τ_f significantly affects the TPI of 1–11. Although τ_f of 2 and 6 were not detected, the sufficiently large ϕ_{ion} was obtained. This is explained by the effect of other factors such as the

molar absorption coefficient of the S_1 (τ_{S_1}) and the rate constant of the ionization of S.

4.2. Important factors for the TPI of methoxy-substituted trans-stilbenes (12–16)

For 12–16, τ_f values were in the range of 32–9100 ps. Among 12–16, *trans*-3,5-dimethoxystilbene (15) has the longest τ_f value. The TPI of 15 seems to be different from those of other methoxy-substituted *trans*-stilbenes (12–14 and 16) because the τ_f value of 15 (9100 ps) is much longer than the laser pulse width (5 ns). This is explained by the "meta effect". It has been reported that the marked difference in excited state behavior of the *trans* isomers of *m*-aminostilbenes versus *p*-aminostilbenes [32]. These aminostilbenes have amino-substituent with electron-withdrawing character at the *meta* position. It is suggested that the twisting about the anilino-styrene bond would result in localization of the positive charge on aniline and the negative charge on styrene. It could result in a larger barrier for twisting about the central bond, which in turn could account for the significantly longer singlet lifetimes for the *meta* isomers. Because methoxy-substituent also has electron-withdrawing character, similar discussion can be applied to 15. Therefore, τ_f of 15 can be observed exceptionally long.

Fig. 3(c) shows that E^{ox} was not a predominant factor for the formation of $S^{\bullet+}$ in the TPI of 12–14 and 16 (open square). Although 13, 14, and 16 have almost the same E^{ox}, ϕ_{ion} altered significantly, indicating that the factors different from the excess energy govern the ϕ_{ion}. Fig. 5 shows that the ϕ_{ion} of 12–14 and 16 depends on τ_f. The small ϕ_{ion} values of 12 and 13 were explained by their relatively short τ_f (approximately 30 ps), while large ϕ_{ion} of 15 and 16 (1.1×10^{-1} and 6.7×10^{-2}) were attributed to their long τ_f (9100 ps and 380 ps, respectively). We have already reported that a CT character of $15(S_1)$ with a long τ_f enhances the S_1–S_n excitation to give $15^{\bullet+}$ in a large ϕ_{ion}. On the other hand, 16 is stabilized in the S_1 state and has long τ_f because of the quinoid-type electron structure of two methoxy substituents [12]. From above reasons, 15 and 16 have the unique photophysical properties in the S_1 states, which are significantly different from other substituted *trans*-stilbenes.

4.3. Importance of the CT electronic character of the S_1 state for the TPI of donor–acceptor-p-substituted trans-stilbenes (17–21)

For 17–21, the peaks and shape of the absorption and fluorescence spectra were different from 1 to 16 (Fig. 1). Table 1 shows that the Stokes shifts of 17–21 in AN are larger than those in CH. The ϕ_{ion} depended not on E^{ox} but on τ_f for the TPI of 17–21 (Figs. 3d and 5; filled square). The excess energy is not a key factor for the TPI of 17–21. It is clear that ϕ_{ion} values for 17–21 were larger than those of other
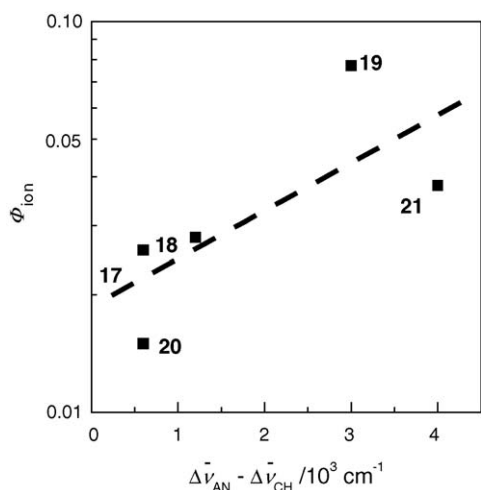
Fig. 6. Plots of the log ϕ_{ion} vs. difference of the Stokes shifts in acetonitrile (AN) and in cyclohexane (CH) ($\Delta\bar{v}_{AN} - \Delta\bar{v}_{CH}$) of donor–acceptor-*p*-substituted *trans*-stilbenes (**17–21**, filled square) during the TPI with the 266-nm laser flash ($F = 0.10\,J\,cm^{-2}$, 5-ns FWHM).

types of *trans*-stilbenes, although they have similar τ_f values to those of other types of *trans*-stilbenes. Fig. 6 shows the plot of log ϕ_{ion} versus the Stokes shift ($\Delta\bar{v}_{AN} - \Delta\bar{v}_{CH}$) for **17–21**. It is clearly observed that ϕ_{ion} increased with an increase in the $\Delta\bar{v}_{AN} - \Delta\bar{v}_{CH}$ value for **17–21**. The existence of the CT excited state has been assumed based on the solvatochromic effects on the absorption and fluorescence spectra and on the τ_f value for **15**(S_1) [12]. The CT excited state of **15**(S_1) was confirmed by the increase of the τ_f value and Stokes shift with increasing of the solvent polarity. Similar increase of the Stokes shift with increasing of the solvent polarity was observed for **17–21**. Therefore, the CT electronic character in the S_1 state is also assumed for **17**(S_1)–**21**(S_1). Similar discussion on the Stokes shift has been reported for the photoionization of aniline derivatives in aqueous solution [33].

4.4. Analysis of the TPI of S by photostationary state within a laser flash

Effects of the parameters of **S**(S_0) and **S**(S_1) on the efficiency of the TPI can be evaluated based on the photostationary state between the S_1 and S_n states of **S** attained within a laser pulse duration of 5 ns. For **S** with short τ_f (<100 ps), [**S**$^{\bullet+}$] can be represented by Eq. (3):

$$[S^{\bullet+}] = \varepsilon_{S_0}\varepsilon_{S_1}l^2I^2[S_0]\tau_f\tau_{S_n}k_it_p \qquad (3)$$

where l is an optical path length, I the laser intensity, t_p the 5 ns of the laser pulse duration, τ_{S_n} the lifetime of **S**(S_n), and k_i represents the rate constant of the ionization of **S**(S_n) [31]. The values of l, I, and t_p are constant, and the product of τ_{S_0} and [S_0] is also constant because the absorbance of **S** in ground state was adjusted to be 1.0 at the excitation laser wavelength. τ_{S_n} can be rewritten as, $\tau_{S_n} = 1/(k_i + k_n)$, where

k_n is the internal conversion rate constant from the S_n state to lower electronic levels. Therefore, [**S**$^{\bullet+}$] should be proportional to $1/(1 + k_n/k_i)$. Since the linear relationship between ϕ_{ion} and [**S**$^{\bullet+}$] (Eq. (2)), it is clear that ε_{S_1}, τ_f, k_i, and/or k_n are the factors for ϕ_{ion} according to the photostationary state analysis.

In Fig. 3(a), no correlation can be found between ϕ_{ion} and E^{ox} when the point of **7** is omitted. If the TPI of **S** would occur directly from the S_1 state, no relation could be obtained between ϕ_{ion} and the photophysical properties of the S_n state, and a horizontal line could be drawn in Fig. 3(a). However, as mentioned above, the existence of the S_n state is confirmed as a discrete level, and the S_n state is involved in the TPI process. Therefore, the log–log plots of ϕ_{ion} versus E^{ox} cannot draw a horizontal line. Among **1–7**, only **5** contains the electron-donating substituent (–CH$_3$) in *para* position. Therefore, the ε_{S_1} value of **5** could significantly differ from those of others containing the electron-withdrawing substituents in *para* position. **12** also contains the electron-donating substituent (–OCH$_3$) in *para* position. Although the E^{ox} values of **5** and **12** were lower than those of **1–4**, the ϕ_{ion} values of **1–5** and **12** were almost the same. It is clearly suggested that the characters of the substituent change the ε_{S_1} values for **1–5** and **12**. On the other hand, **6** and **7** contain the strong electron-withdrawing substituents (–CF$_3$ and –CN in *para* position, respectively). Fig. 3(b) represents the plots for all di-*p*-substituted **S** (**8–11**). Comparing **8–10** to **11**, the τ_f and Stokes shift values were almost the same, but E^{ox} of **8–10** (1.20–1.27 V) were higher than that of **11** (1.02 V). The ϕ_{ion} value of **11** is higher than those of **8–10** ((1.8–2.1) × 10^{-2}). It is assumed that the magnitude of excess energy for the ionization, which is the difference between the excitation energy of S_n state and I.P., could affect the photophysical properties of the S_n state such as k_i and k_n, and therefore, ϕ_{ion} values. For **12–16**, ϕ_{ion} depended on the τ_f value. In particular for **15** and **16**, it is clear that the long lifetime affects the ϕ_{ion}, suggesting the effect of τ_f is more important factor than k_i or ε_{S_1} for the TPI of **12–16**. For **17–21**, the dependence of ϕ_{ion} on τ_f seems to be significant although the τ_f and E^{ox} values were very similar. The k_i and k_n values are expected to be similar for **17–21** because of the similar E^{ox} values. Therefore, it is suggested that the ε_{S_1} value is important for ϕ_{ion} of **17–21**. This is explained by the CT character of the S_1 state. Comparing **17–21** to **12**, E^{ox} and τ_f were similar, but the ϕ_{ion} values at 266 nm of **17–21** ((1.5–7.7) × 10^{-2}) were several fold larger than that of **12** (1.0 × 10^{-2}). It is explained that the ϕ_{ion} value depends strongly on the ε_{S_1} value for the TPI of **17–21**. The effect of τ_f value is suggested to be small for **17–21**.

Thus, TPI of **S** is governed by several factors, therefore, the different slopes for each types of **S** as shown in Fig. 5 are probably explained by the effects of other factors such as ε_{S_1}, k_n, and k_i. Similarly, such factors may affect on the values coming off from the relations as shown in Figs. 3 and 6.
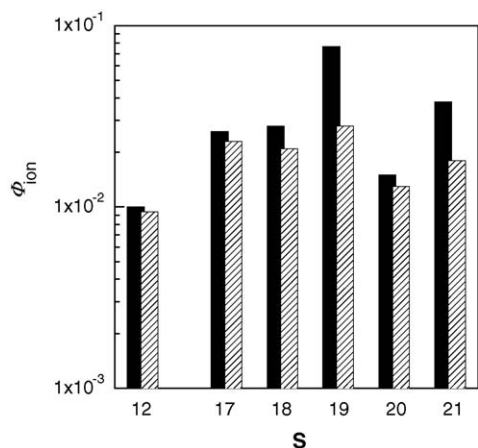
Fig. 7. Comparison of ϕ_{ion} during the TPI with the 266-nm (solid bars) and 355-nm (shaded bars) lasers for *trans*-4-methoxystilbene (**12**) and donor–acceptor-*p*-substituted *trans*-stilbenes (**17–21**).

4.5. Laser wavelength dependence on the TPI of trans-4-methoxystilbene (12) and donor–acceptor-p-substituted trans-stilbene (17–21)

Fig. 7 shows log ϕ_{ion} during the TPI of **12** and **17–21** with the 266- or 355-nm laser flashes. These **S** have absorption at 266 and 355 nm. The τ_f values are almost the same (approximately 30 ps). When the excitation wavelength was 266 nm, the ϕ_{ion} values of **17–21** were larger than that of **12**, which is explained by CT electronic character of **17**(S_1)–**21**(S_1) in S_1 states. In the case of the 355-nm excitation (5 ns, 0.31 J cm^{-2}), the ϕ_{ion} values of **12**, **17**, **18**, and **20** slightly decreased compared to the 266-nm excitation, while those of **19** and **21** decreased considerably. It seems that the excess energy does not change significantly with changing the excitation wavelength because of the relatively low E^{ox} of **12** and **17–21**. Because the ϕ_{ion} values changed only a little for the TPI of **12** with the excitation wavelength at 266 and 355 nm, it is expected that TPI of **17–21**, with almost the same E^{ox} values, would not be significantly affected by changing the excitation wavelength. Therefore, the results suggest that **19**(S_1) and **21**(S_1) have smaller ε_{S_1} values at 355 nm than those at 266 nm, while those of **12**, **17**, **18**, and **20** are only slightly smaller at 355 nm than those at 266 nm. Consequently, the wavelength-dependence is clearly observed in the TPI of **19** and **21**, while that is weak in the TPI of **12**, **17**, **18**, and **20**.

4.6. Importance of photophysical properties of the S₁ state for the TPI of S (1–21)

The mechanism of the TPI of **S** is explained as shown in Scheme 2, where IC is internal conversion, Fl is fluorescence, ε_{S_0} and ε_{S_1} (or ε_{CT}) are the molar absorption coefficients of the S_0 and S_1 (or CT) states, respectively. For **1–16**, τ_f has a significant effect. The smaller ϕ_{ion} values for **12** and **13** are

explained by their short τ_f. **15** and **16** have long τ_f, because of the stabilization in the S_1 states due to the formation of CT state and quinoid-type structure, respectively [12]. The TPI of donor–acceptor-*p*-substituted *trans*-stilbenes (**17–21**) depended on τ_f and ε_{S_1}. The ϕ_{ion} of **17–21** increased with an increase in the Stokes shift. It is suggested that the TPI of **17–21** occurs effectively due to the increase of ε_{S_1} value. It seems this increase of ε_{S_1} is related to the CT character of **17–21** occurred in the S_1 state. It is also suggested that the ε_{CT} values of **19** and **21** are different from those of **17**, **18**, and **20** at the excitation wavelengths. Although ε_{CT} of **17**, **18**, and **20** are similar at 266 and 355 nm, those of **19** and **21** at 266 nm are much larger than those at 355 nm. Consequently, the TPI of **S** strongly depends on the photophysical properties of the intermediate S_1 state.

Effects of photophysical properties of the intermediate singlet excited states on the TPI efficiency have been extensively studied. Blanchet et al. reported the first 287-nm excitation from the S_0 state to the S_2 state which decays to the S_1 state, and second 235- or 352-nm excitation from the S_1 state to give photoelectron through the ionization of all-*trans* 2,4,6,8-decatetraene using pump-probe time-resolved photoelectron spectroscopy [34]. Thus, it is summarized that the electronic configuration change of the intermediate singlet excited states affects the TPI efficiency. This is consistent with the results for the TPI of **S**.

5. Conclusions

S$^{\bullet+}$ was generated from the TPI of **S** in AN with irradiation of a Nd^{3+}:YAG laser pulse (266 or 355 nm, 5 ns) at sufficiently high F (0.10 and 0.31 J cm^{-2}, respectively). It is clearly indicated that τ_f has a significant effect on the TPI of non-substituted (**1**), mono-*p*-substituted (**2–7**), di-*p*-substituted (**8–11**), and methoxy-substituted *trans*-stilbenes (**12–16**). For the TPI of donor–acceptor-*p*-substituted *trans*-stilbenes (**17–21**), the large ϕ_{ion} value was obtained even though they have short τ_f, suggesting that the CT electronic character in the S_1 state significantly affects the TPI of **17–21**. It was also shown that ϕ_{ion} depended on the excitation wavelength, suggesting that ε_{S_1} is an important factor for the TPI. Thus, it is concluded that the TPI of **S** depends strongly on the photophysical properties of the S_1 state. It should be noted that **S** can be designed to have both donor and acceptor substituents in order to generate **S**$^{\bullet+}$ in a high yield.

Appendix A. Supplementary data

Supplementary data associated with this article can be found, in the online version, at doi:10.1016/j.jphotochem.2005.08.005.

References

[1] A. Kellmann, F. Tfibel, Chem. Phys. Lett. 69 (1980) 61.
[2] Y. Taniguchi, Y. Nishida, N. Mataga, Bull. Chem. Soc. Jpn. 45 (1972) 2923.
[3] J.T. Richards, G. West, J.K. Thomas, J. Phys. Chem. 74 (1970) 4137.
[4] Y. Mori, A. Yoneda, H. Shinoda, T. Kitagawa, Chem. Phys. Lett. 183 (1991) 584.
[5] J.L. Faria, S. Steenken, J. Phys. Chem. 97 (1993) 1924.
[6] M.A. Fox, Chem. Rev. 79 (1979) 253.
[7] S.S. Shukla, J.F. Rusling, J. Phys. Chem. 89 (1985) 3353.
[8] H.J. Shine, D.C. Zhao, J. Org. Chem. 55 (1990) 4086.
[9] D.T. Breslin, M.A. Fox, J. Phys. Chem. 98 (1994) 408.
[10] J. Oberlé, E. Abraham, A. Ivanov, G. Jonusauskas, C. Rullière, J. Phys. Chem. 100 (1996) 10179.
[11] T. Nakabayashi, S. Kamo, H. Sakuragi, N. Nishi, J. Phys. Chem. A 105 (2001) 8605.
[12] M. Hara, S. Tojo, T. Majima, J. Photochem. Photobiol. A 162 (2004) 121.
[13] G.D. Diana, P.M. Carabateas, R.E. Johanson, G.L. Williams, F. Pancic, J.C. Collins, J. Med. Chem. 21 (1978) 889.
[14] C.S. Wood, F.B. Mallory, J. Org. Chem. 29 (1964) 3373.
[15] A.K. Singh, S. Kanvah, J. Chem. Soc, Perkin Trans. 2 (2001) 395.
[16] M. Shi, B. Xu, J. Org. Chem. 67 (2002) 294.
[17] L. Engman, J. Org. Chem. 49 (1984) 3559.
[18] M. Oki, Y. Urushibara, Bull. Chem. Soc. Jpn. 25 (1952) 109.
[19] D. Molho, J. Coillard, Bull. Soc. Chim. France (1956) 78.
[20] J.I.G. Cadogan, E.G. Duell, P.W. Inward, J. Chem. Soc. (1962) 4164.
[21] R.F.B. Cox, J. Am. Chem. Soc. 62 (1940) 3512.
[22] V. Papper, D. Pines, G. Linkhtenshtein, E. Pines, J. Photochem. Photobiol. A 111 (1997) 87.
[23] S.M. Halaas, K. Okyne, A.J. Fry, Electrichem. Acta 48 (2003) 1837.
[24] L. Meites, P. Zuman, CRC Handbook Series in Organic Electrochemistry, CRC Press, Cleveland, 1975.
[25] F. Wilkinson, C. Tsiamis, J. Am. Chem. Soc. 105 (1983) 767.
[26] A. Singh, H.D. Gesser, A.R. Scott, Chem. Phys. Lett. 2 (1968) 271.
[27] T. Majima, S. Tojo, A. Ishida, S. Takamuku, J. Phys. Chem. 100 (1996) 13615.
[28] I.P. Bell, M.A.J. Rodgers, H.D. Burrows, J. Chem. Soc., Faraday Trans. 73 (1) (1977) 315.
[29] T. Majima, M. Fukui, A. Ishida, S. Takamuku, J. Phys. Chem. 100 (1996) 8913.
[30] F.D. Lewis, A.M. Bedell, R.E. Dykstra, J.E. Elbert, I.R. Gould, S. Farid, J. Am. Chem. Soc. 112 (1990) 8055.
[31] M. Hara, S. Tojo, M. Fujitsuka, T. Majima, Chem. Phys. Lett. 393 (2004) 338.
[32] F.D. Lewis, J.-S. Yang, J. Am. Chem. Soc. 119 (1997) 3834.
[33] F. Saito, S. Tobita, H. Shizuka, J. Photochem. Photobiol. A 106 (1997) 119.
[34] V. Blanchet, M.Z. Zgierski, T. Seideman, A. Stolow, Nature 401 (1999) 52.